

journal homepage: <http://civiljournal.semnan.ac.ir/>

Effect of Steel Confinement on Behavior of Reinforced Concrete Frame

A. Hemmati^{1*} and Sh. Mojaddad²

1. Assistant Professor, Seismic Geotechnical and High Performance Concrete Research Center, Department of Civil Engineering, Semnan Branch, Islamic Azad University, Semnan, Iran

2. Department of Civil Engineering, Semnan Branch, Islamic Azad University, Semnan, Iran

Corresponding author: ali.hemmati@semnaniau.ac.ir

ARTICLE INFO

Article history:

Received: 23 January 2018

Accepted: 11 June 2018

Keywords:

Confinement,

Ductility,

Frame,

Steel Reinforcement,

Tension Damage.

ABSTRACT

The strength and ductility of concrete are improved under multi-axial compressive stress due to confinement effect. Some effective parameters for concrete confinement are longitudinal and transverse steel reinforcement. Some stress-strain relations for confined concrete with steel reinforcement have been proposed by different researchers. In this paper, various stress strain models with considering the steel confinement effect are reviewed briefly and used for simulating the lateral behavior of on an experimental reinforced concrete frame. Envelope curves, tension damage, yielding patterns, ductility ratio and energy absorption of the frames are discussed. Results from the finite element analysis compared with experimental findings show that in the case of lateral load and displacement, the analytical models which were presented by Fafitis et al. and Muguruma et al. had more compatibility with experimental results and the difference is less than 10%. Energy absorption of the model which was proposed by Khaje Samani & Attard had the most compatibility with experimental results and difference is about 1%.

1. Introduction

Confinement in concrete concluded to higher strains with lower degradation in softening part of compressive stress-strain curve of this material. Steel reinforcement, steel jacketing, FRP and some other materials can perform as a confining material for concrete. As it shown

in Fig. 1, both steel and FRP confined concrete have more compressive strength and ultimate strain than those of unconfined concrete and strain softening occurs with slower rate. Moreover, FRP confined concrete has a part of strain hardening in its stress-strain curve [1, 2]. Longitudinal and transverse reinforcements are effective

parameters for concrete confinement as it shown in Fig. 2 [3].

Many studies have been performed on behavior of confined concrete and its applications in structural modeling. Suzuki et al. developed a stress-strain model of high strength concrete confined by rectangular ties and the finite element findings were verified by experimental results [4].

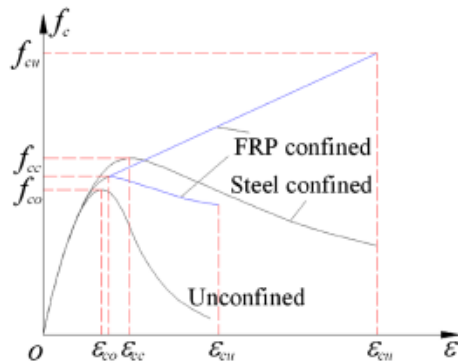


Fig. 1. Effect of confinement on stress-strain curve of concrete [2].

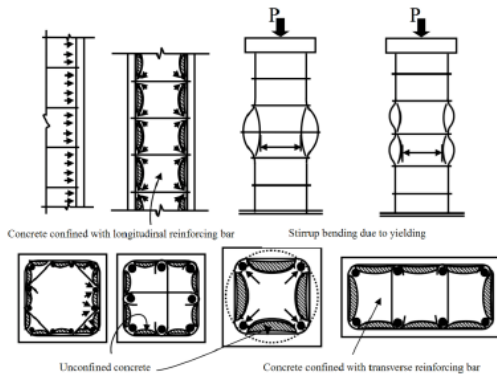


Fig. 2. Effect of confinement on stress-strain curve of concrete [3].

A model for damage analysis of confined and unconfined concrete was developed by Cao and Ronagh [5]. Sadeghi proposed an analytical nonlinear stress-strain model and damage index for confined and unconfined concrete to simulate reinforced concrete structures under seismic loading [6]. Kheyroddin and Naderpour presented a model for predicting the compressive

strength of confined concrete in CCFST columns [7].

Efficiency of stress-strain models of confined concrete with and without steel jacketing to reproduce the experimental results was investigated by Campoine et al. In this research, the reliability of some constitutive models for confined concrete was examined and verified by experimental data [8]. The effect of confinement on the collapse probability of reinforced concrete frames subjected to earthquakes was studied by Laresen et al. The results showed statistically significant effect of confinement on the collapse probability of reinforced concrete frames [9].

2. Stress-Strain Models for Confined Concrete with Steel Reinforcements

2.1. Blume et al. (1961)

Presented equation for confined concrete is shown in Fig. 3 and Eq. (1).

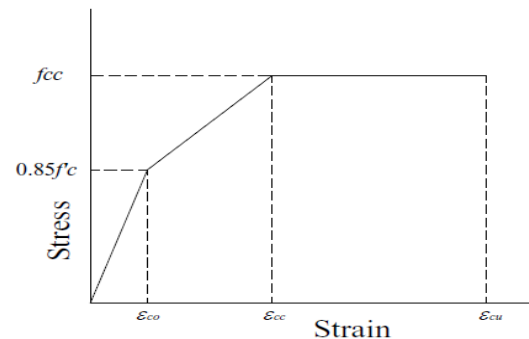


Fig. 3. Stress-strain curve of confined concrete [10].

$$f_{cc} = 0.85f'_c + 4.1 \frac{A_{st} f_{yh}}{sh}$$

$$\epsilon_{c0} = \frac{0.22f'_c + 400 \text{ psi}}{10^6 \text{ psi}} \quad (1)$$

$$\epsilon_{cc} = 5\epsilon_y$$

$$\epsilon_{cu} = 5\epsilon_{su}$$

Where, A_{st} and f_{yh} are section area and yielding stress of transverse steel reinforcements respectively. As it shown, this stress-strain curve includes three linear sections without any softening part and the confinement effect of longitudinal reinforcement is ignored.

2.2. Soliman and Yu (1967)

Presented equation for confined concrete is shown in Fig. 4 and Eq. (2).

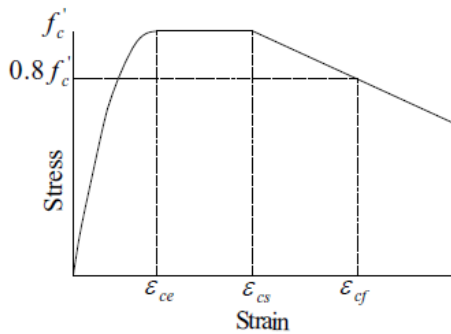


Fig. 4. Stress-strain curve of confined concrete [11].

$$f_{cc} = 0.9f'_c + (1 + 0.05q)$$

$$q = \left(1.4 \frac{A_{cc}}{A_c} - 0.45 \right) \frac{A_{st}(s_0 - s)}{A_{st}s + 0.0028Bs^2}$$

$$\epsilon_{cc} = 0.55f_{cc} \times 10^{-6}$$

$$\epsilon_{cs} = 0.0025(1 + q)$$

$$\epsilon_{cf} = 0.0045(1 + 0.85q) \tag{2}$$

As it shown, this stress-strain curve includes four sections with softening part and the confinement effect of longitudinal reinforcement is ignored. Moreover, the strain corresponding to the 0.85 of compressive strength (f'_c), has been considered as ultimate compressive strain of confined concrete.

2.3. Kent and Park (1971)

Presented equation for confined concrete is shown in Fig. 5 and Eq. (3).

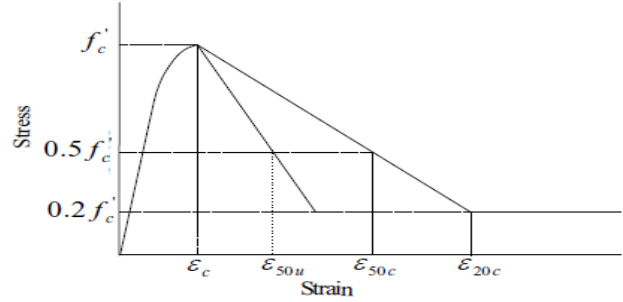


Fig. 5. Stress-strain curve of confined concrete [12].

$$f_c = f'_c \left[\frac{2\epsilon_c}{\epsilon_{c0}} - \left(\frac{\epsilon_c}{\epsilon_{c0}} \right)^2 \right]$$

$$f_c = f'_c [1 - Z(\epsilon_c - \epsilon_{c0})]$$

$$\epsilon_{50u} = \frac{3 + 0.002f'_c}{f'_c - 1000}$$

$$\rho_s = \frac{2(h+b)A_{st}}{hbs} \tag{3}$$

$$\epsilon_{50h} = \epsilon_{50c} - \epsilon_{50u}$$

$$\epsilon_{50h} = \frac{3}{4} \rho_s \sqrt{\frac{b}{s}}$$

$$Z = \frac{0.5}{\epsilon_{50h} + \epsilon_{50u} - \epsilon_{c0}}$$

This stress-strain curve includes two sections with softening part and the confinement effect of longitudinal reinforcement is ignored.

2.4. Valenas et al. (1977)

Presented equation for confined concrete in ascending in descending parts is shown in Fig. 6 and Eq. (4) and Eq. (5) respectively.

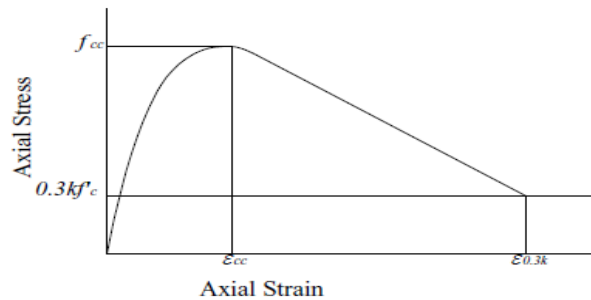


Fig. 6. Stress-strain curve of confined concrete [13].

$$\frac{f_c}{f'_c} = k[1 - Z\varepsilon_{cc}(x-1)] \quad \varepsilon_c \leq \varepsilon_c \leq \varepsilon_{0.3k}$$

$$\frac{f_c}{f'_c} = 0.3k \quad \varepsilon_c \geq \varepsilon_{0.3k}$$

$$x = \frac{\varepsilon_c}{\varepsilon_{cc}} \quad (4)$$

$$f_{cc} = kf'_c$$

$$\frac{f_c}{f'_c} = \frac{\frac{E_c \varepsilon_{cc}}{f'_c} x - kx^2}{1 + \left(\frac{E_c \varepsilon_{cc}}{kf'_c} - 2 \right) x} \quad \varepsilon_{cc} \geq \varepsilon_c$$

$$k = 1 + 0.0091 \left[1 - 0.245 \frac{s}{h} \right] \frac{\left[\rho + \frac{d_{st}}{d'_s} \rho_l \right] f_{yh}}{f'_c}$$

$$\varepsilon_{cc} = 0.0024 + 0.005 \left[1 - \frac{0.734s}{h} \right] \frac{\rho f_{yh}}{\sqrt{f'_c}} \quad (5)$$

$$Z = \frac{0.5}{\frac{3}{4} \rho_s \sqrt{\frac{h}{s}} + \left[\frac{3 + 0.002 \sqrt{f'_c}}{f'_c - 1000} \right] - 0.002}$$

This stress-strain curve includes two sections with softening part and the confinement effect of both longitudinal and transverse reinforcements is considered.

2.5. Muguruma et al. (1978)

Presented equation for confined concrete in three parts is shown in Fig.7 and Eq. (6). $\left(\frac{kgf}{cm^2} \right)$.

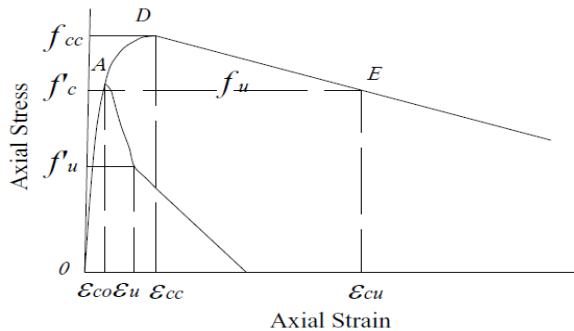


Fig. 7. Stress-strain curve of confined concrete [14].

OA part:

$$f_c = E_i \varepsilon_c + \frac{f'_c - E_i \varepsilon_{c0}}{\varepsilon_{c0}^2} \varepsilon_c^2$$

AD part:

$$f_c = f_{cc} + \frac{(\varepsilon_c - \varepsilon_{cc})^2}{(\varepsilon_{c0} - \varepsilon_{cc})^2} (f'_c - f'_{cc})$$

DE part:

$$f_c = f_{cc} + \frac{f_u - f_{cc}}{\varepsilon_{cu} - \varepsilon_{cc}} (\varepsilon_c - \varepsilon_{cc})$$

$$f_u = \frac{2(\bar{s} - f_{cc} \varepsilon_{cc})}{\varepsilon_{cc} + \varepsilon_{cu}} \quad (6)$$

$$\varepsilon_u = 0.00413 \left(1 - \frac{f'_c}{2000} \right)$$

$$C_c = \rho_s \frac{\sqrt{f_{yh}}}{f'_c} \left(1 - 0.5 \frac{s}{W} \right)$$

In this research, some equations were presented for circular and square columns. The confinement effect of longitudinal reinforcement is ignored in these equations.

2.6. Scott et al. (1982)

Presented equation for confined concrete in three parts is shown in Eq. (7).

$$f_c = kf'_c \left(\frac{2\varepsilon_c}{0.002k} - \left(\frac{\varepsilon_c}{0.002k} \right)^2 \right) \quad (7)$$

Where, k is a parameter related to amount of and yielding stress of steel reinforcements and compressive strength of concrete [15].

2.7. Sheikh and Uzumeri (1982)

Presented equation for confined concrete in three parts is shown in Fig.8 and Eq. (8).

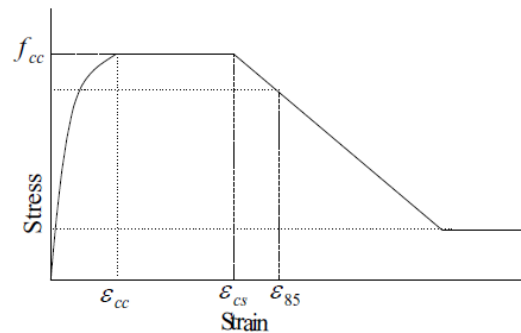


Fig. 8. Stress-strain curve of confined concrete [16].

$$f_{cc} = k_s f_{cp} \quad f_{cp} = k_p f'_c \quad k_p = 0.85$$

$$k_s = 1 + \frac{2.73b^2}{P_{occ}} \left[\left(1 - \frac{nc^2}{5.5b^2} \right) \left(1 - \frac{s}{2b} \right)^2 \right] \sqrt{\rho_s f'_{st}}$$

$$\varepsilon_{cc} = 0.55 k_s f'_c \times 10^{-6}$$

$$\varepsilon_{cc} = \varepsilon_{c0} \left(1 + \frac{0.81}{c} \left(1 - 5 \left(\frac{s}{b} \right)^2 \right) \frac{\rho_s f'_{st}}{\sqrt{f'_c}} \right) \quad (8)$$

$$\varepsilon_{85} = 0.225 \rho_s \sqrt{\frac{b}{s}} + \varepsilon_{cs}$$

$$Z = \frac{0.5}{\frac{3}{4} \rho_s \sqrt{\frac{b}{s}}}$$

The confinement effect of longitudinal reinforcement is ignored in these equations.

2.8. Park et al. (1982)

Presented equation for confined concrete in three parts is shown in Fig.9 and Eq. (9) and eq.10.

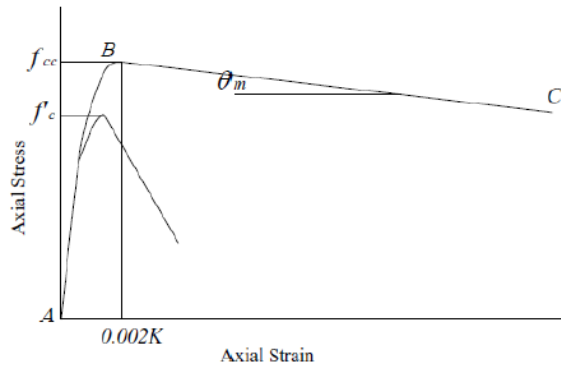


Fig. 9. Stress-strain curve of confined concrete [17].

For ascending part:

$$f_c = k f'_c \left[\frac{2\varepsilon_c}{0.002k} - \left(\frac{\varepsilon_c}{0.002k} \right)^2 \right] \quad (9)$$

For descending part:

$$f_c = k f'_c [1 - Z_m (\varepsilon_c - \varepsilon_{c0})] \geq 0.2 k f'_c$$

$$Z_m = \frac{0.5}{\frac{3 + 0.29 f'_c}{145 f'_c - 1000} + \frac{3}{4} \rho_s \sqrt{\frac{b}{s}} - 0.002k} \quad (10)$$

$$k = 1 + \frac{\rho_s f_{yh}}{f'_c}$$

The confinement effect of longitudinal reinforcement is ignored in these equations.

2.9. Fafitis and Shah (1985)

Presented equation for confined concrete in descending part is shown in Eq. (11).

$$f_c = f'_c \exp \left[-k (\varepsilon_c - \varepsilon_{cc})^{1.15} \right] \quad (11)$$

Where, k is a parameter related to amount, spacing and yielding stress of transverse reinforcements for both circular and square columns [18].

2.10. Yong et al. (1988)

Presented equation for confined concrete in three parts is shown in Fig.10 and Eq. (12).

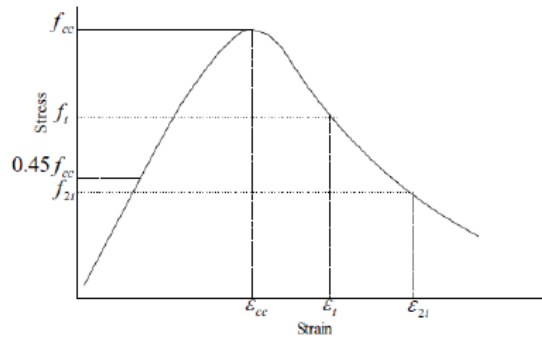


Fig. 10. Stress-strain curve of confined concrete [19].

$$f_{cc} = k f'_c$$

$$\varepsilon_{cc} = 0.00265 + \frac{0.0035 \left(1 - \frac{0.734s}{h} \right) (\rho_s f_{yh})^{2/3}}{\sqrt{f'_c}}$$

$$k = 1 + 0.0091 \left(1 - \frac{0.245s}{h} \right) \left(\rho_s + \frac{nd_{st}}{8sd'_s} \rho_l \right) \frac{f_{yh}}{\sqrt{f'_c}} \quad (12)$$

$$f_i = f_{cc} \left[0.25 \left(\frac{f'_c}{f_{cc}} \right) + 0.4 \right]$$

$$\varepsilon_i = k \left[1.4 \left(\frac{\varepsilon_{cc}}{k} \right) + 0.0003 \right]$$

$$f_{2i} = f'_c \left[0.025 \left(\frac{f_{cc}}{1000} \right) - 0.065 \right] \geq 0.3 f_{cc}$$

The confinement effect of longitudinal reinforcement is ignored in these equations.

2.11. Mander et al. (1988)

Presented equation for confined concrete in three parts is shown in Fig.11 and Eq. (13).

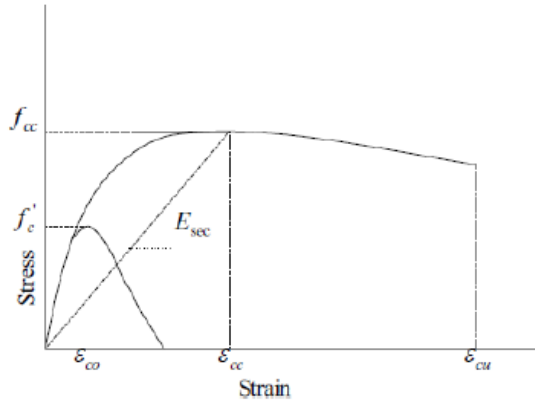


Fig. 11. Stress-strain curve of confined concrete [20].

$$f_{cc} = f'_c \left[-1.254 + 2.254 \sqrt{1 + \frac{7.94 f'_l}{f'_c} - 2 \frac{f'_l}{f'_c}} \right] \quad (13)$$

$$\varepsilon_{cc} = \varepsilon_{c0} \left[1 + 5 \left(\frac{f_{cc}}{f'_c} - 1 \right) \right]$$

Where, f_l is a parameter related to amount, type and yielding stress of transverse reinforcement.

2.10. Fuji et al. (1988)

Presented equation for confined concrete in three parts is shown in Fig.12 and Eq. (14).

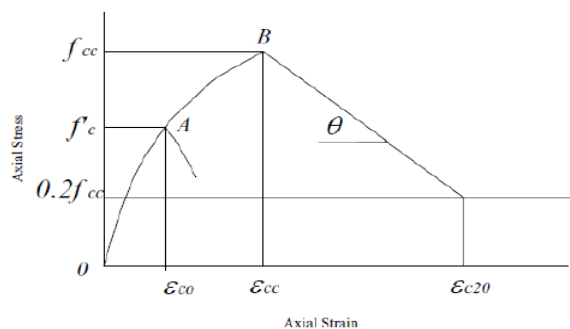


Fig. 12. Stress-strain curve of confined concrete [21].

$$f_c = E_i \varepsilon_c + \frac{f'_c - E_i \varepsilon_{c0}}{\varepsilon_{c0}^2} \varepsilon_c^2 \quad 0 \leq \varepsilon_c \leq \varepsilon_{c0}$$

$$f_c = f_{cc} + \frac{(\varepsilon_c - \varepsilon_{cc})^3}{(\varepsilon_{c0} - \varepsilon_{cc})^3} (f'_c - f_{cc}) \quad \varepsilon_{c0} \leq \varepsilon_c \leq \varepsilon_{cc} \quad (14)$$

$$f_c = f_{cc} - \theta(\varepsilon_c - \varepsilon_{cc}) \quad \varepsilon_{cc} \leq \varepsilon_c \leq \varepsilon_{c20}$$

$$f_c = 0.2 f_{cc} \quad \varepsilon_{c20} \leq \varepsilon_c$$

Where, θ is a parameter related to amount, type and yielding stress of transverse reinforcement.

2.11. Saatcioglu and Razavi (1992)

Presented equation for confined concrete in three parts is shown in Fig.13 and Eq. (15).

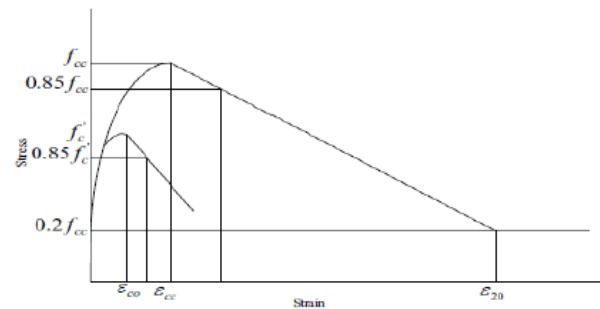


Fig. 13. Stress-strain curve of confined concrete [22].

$$f_{cc} = f'_c + k_1 f_l \quad (15)$$

Where, f_l and k_1 are two parameters related to amount, type and yielding stress of transverse and longitudinal reinforcements.

2.12. Cusson and Paoltre (1995)

Presented equation for confined concrete in descending part is shown in Fig. 14 and Eq. (16).

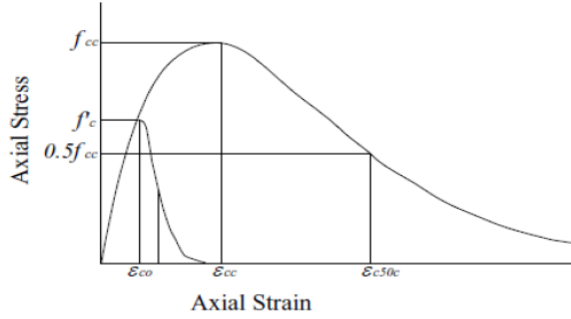


Fig. 14. Stress-strain curve of confined concrete [23].

$$f_c = f_{cc} \exp\left(k_1(\varepsilon_{c50c} - \varepsilon_{cc})^{k_2}\right) \quad (16)$$

Where, k_1 and k_2 is two parameters related to amount of steel reinforcements.

2.12. Hoshikuma et al. (1997)

Presented equation for confined concrete in descending part is shown in Eq. (17).

$$f_c = f_{cc} - E_{des}(\varepsilon_c - \varepsilon_{cc}) \quad (17)$$

Where, E_{des} is a parameter related to amount, spacing and yielding stress of transverse reinforcements for both circular and square columns [24].

2.12. Binici (2005)

Presented equation for confined concrete in three parts is shown in Fig.15 and Eq. (18).

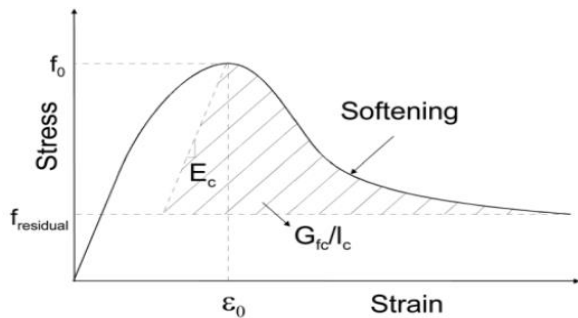


Fig. 15. Stress-strain curve of confined concrete [25].

$$f = E_c \varepsilon \quad \varepsilon \leq \varepsilon_{1e}$$

$$f = f_{1e} + (f_0 - f_{1e}) \frac{r \left(\frac{\varepsilon - \varepsilon_{1e}}{\varepsilon_0 - \varepsilon_{1e}} \right)}{r - 1 + \left(\frac{\varepsilon - \varepsilon_{1e}}{\varepsilon_0 - \varepsilon_{1e}} \right)^2} \quad \varepsilon_{1e} \leq \varepsilon \leq \varepsilon_0$$

$$f = f_{residual} + (f_0 - f_{residual}) \exp\left[-\left(\frac{\varepsilon - \varepsilon_0}{\alpha}\right)^2\right] \quad \varepsilon \geq \varepsilon_0$$

(18)

Where, r is a parameter related to amount, type and yielding stress of transverse and longitudinal reinforcements.

2.13. Bouafia et al. (2010)

Presented equation for confined concrete in three parts is shown in Fig.16 and Eq. (19).

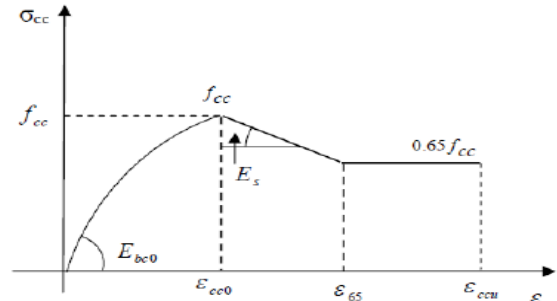


Fig. 16. Stress-strain curve of confined concrete [26].

$$\sigma = f_{cc} \times \frac{k_c \times \bar{\varepsilon}_c + (k'_c - 1) \times \bar{\varepsilon}_c^2}{1 + (k_c - 2) \times \bar{\varepsilon}_c + k'_c \times \bar{\varepsilon}_c^2} \quad 0 \leq \varepsilon_c \leq \varepsilon_{cc0}$$

$$\bar{\varepsilon}_c = \frac{\varepsilon_c}{\varepsilon_{cc0}} \quad \varepsilon_{cc0} = \varepsilon_{c0} \times \left[1 + 5 \left(\frac{f_{cc}}{f_{c0}} - 1 \right) \right]$$

$$k_c = \frac{E_{bc0} \times \varepsilon_{cc0}}{f_{cc}} \quad E_{bc0} = 11000 \sqrt[3]{f_{cc}} \quad k'_c = k_c - 1 \quad (19)$$

$$\sigma_{cc} = f_{cc} - E_s(\varepsilon_c - \varepsilon_{cc0}) \quad \varepsilon_{cc0} \leq \varepsilon_c \leq \varepsilon_{c65}$$

$$E_s = \frac{6 \times f_{c0}^2}{k_e \times \rho_s \times f_{yh}}$$

The confinement effect of longitudinal reinforcement has been ignored in these equations.

2.14. KhajeSamani and Attard (2012)

Presented equation for confined concrete in descending part is shown in Fig.17 and Eq. (20).

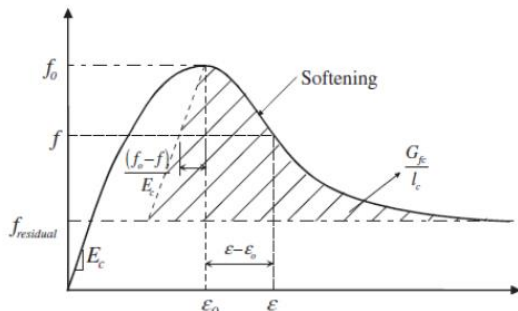


Fig. 17. Stress-strain curve of confined concrete [27].

$$\frac{f}{f_0} = \frac{f_{residual}}{f_0} + \left(1 - \frac{f_{residual}}{f_0}\right) \left(\frac{f_{ic}}{f'_c}\right) \left(\frac{\varepsilon - \varepsilon_0}{\varepsilon_i - \varepsilon_0}\right) \quad (20)$$

Where, $f_{residual}$ is a parameter related to amount transverse reinforcement.

As it discussed, arrangement or yielding stress or space of the transverse reinforcement are considered in the whole above equations but the effect of longitudinal reinforcement in confined concrete is ignored in some models.

In this paper a reinforced concrete frame that has been tested experimentally by Tawfik et al. is selected and modeled by ABAQUS software. Analytical frames are investigated using these above equations and the results verified with experimental data.

3. Experimental Program and Analytical Investigations

Dimensions and reinforcement details of the experimental specimen, lateral loading protocol and test set up are shown in Fig.18, Fig.19 and Fig.20 respectively. All of the dimensions are in mm. compressive strength of concrete was 30 MPa. Yielding stress of longitudinal and transverse reinforcement were 360 MPa and 240 MPa respectively [28].

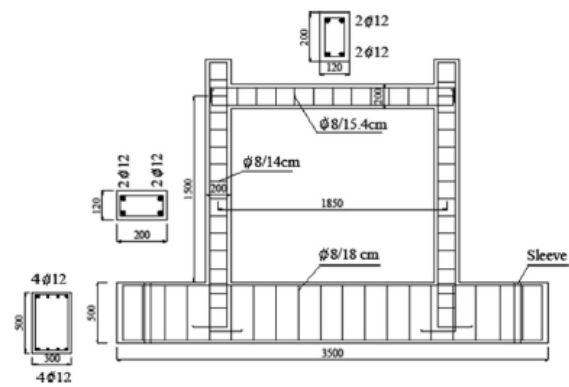


Fig. 18. Experimental frame [28].

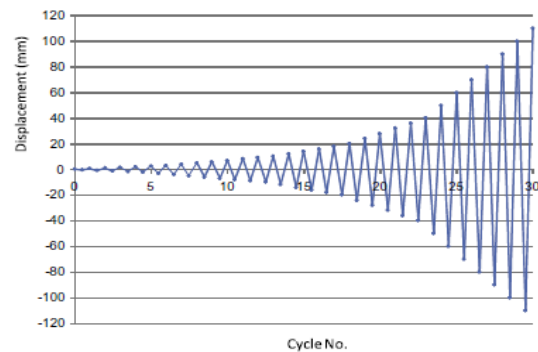


Fig. 19. Loading protocol [28].

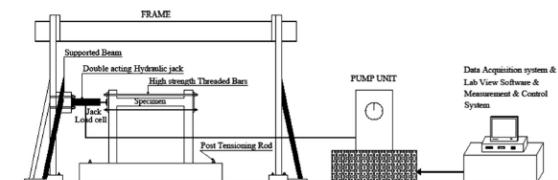


Fig. 20. Test set up [28].

ABAQUS is strong FEM-based engineering software used for performing non-linear

analyses. In this type of analysis, ABAQUS automatically selects appropriate load increments and convergence tolerances and continually adjusts them during the analysis to ensure that a highly accurate solution is obtained. For concrete and steel modeling, a 3D 8-node linear iso-parametric element with reduced integration (C3D8R) and a 2-node linear tetrahedral element (C3D2) are used, respectively. Each node in the 8-node element and truss element has three degrees of freedom. These elements are capable of modeling non-linear behaviors of concrete and steel.

For evaluation of an appropriate value of ultimate tensile strain of the concrete (ε_{tu}) and elimination of the mesh size dependency phenomenon, Shayanfar et al. presented the following equation [29].

$$\varepsilon_{tu} = 0.004e^{-0.008h} \text{ Eq.21.}$$

Where, h is the width of the element (mm).

In this paper, some analytical frames are modeled and lateral behavior of these frame under the loading protocol investigated. In these analytical frames, confined concrete with steel reinforcement is modeled by various stress-strain equations which were presented in section 2 and consequently, the envelope curves of these models are presented and compared with each other and experimental results. These envelope curves are shown in Fig.21. Moreover, it must be noted that the experimental envelope curve is shown by bold solid line in this figure.

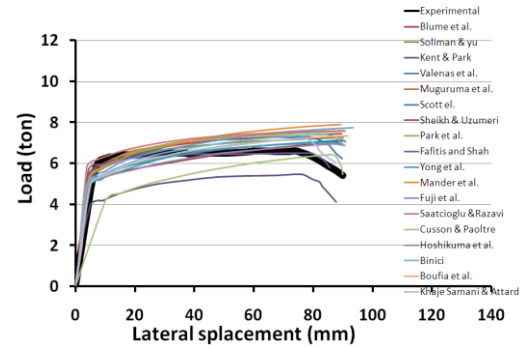


Fig. 21. Envelope curves of analytical reinforced concrete models with different stress-strain equations.

As it shown, the initial stiffness of the whole analytical frames (except Cusson and Paoltre model) is more than that of experimental specimen. Moreover, the envelope curves of Soliman & Yu, Mugurama et al., Sheikh & Uzumeri, Mander et al., Fuji et al., Saatcioglu & Razavi and Boufia models are ascending and have not a softening part. In these models, when the compressive strain of concrete in an element reach to its corresponding ultimate magnitude (ε_{cu}), the nonlinear analysis is stopped and the maximum displacement defined.

The stress-strain relation which was proposed by Kent & Park, Scout et al., Fafitis and Shah, Cusson & Paoltre, Binici and Attard includes two separate parts of ascending and descending in their envelope curves. In the other hand, in these analytical models, softening part of the envelope curve occurs. In softening part of these envelope curves, when the lateral load reach to 85% of the maximum load (P_u), the nonlinear analysis is stopped and the maximum displacement defined.

In the case of proposed models by Blume et al., Valenas et al., Yong et al. and Hoshikuma et al., envelope curves includes two sections but the softening parts in these envelope curves are very small and the first criteria is used for defining the maximum displacement of these frames.

Summary of these analytical results are presented in Table 1.

Table 1. Summary of analytical results.

Model	Δ_y (mm)	P_y (ton)	Δ_u (mm)	P_u (ton)	$\mu = \frac{\Delta_u}{\Delta_y}$	E (ton.mm)
Experimental	8.9	6	90	6.6	10.1	554.8 7
Blume et al.	9	5.31	89.6	7.08	9.95	549.2 3
Soliman & Yu	10.5	5.9	90.1	7.26	8.58	591.2 5
Kent & Park	9.5	4.21	87.7	5.46	9.23	429.0 1
Valenas et al.	10.2	5.3	90.84	7.14	8.90	572.7 5
Muguruma et al.	9	6	90.7	7.58	10.07	621
Scott et al.	9	5.6	89.8	7.28	9.97	594.6 4
Sheikh & Uzumeri	9.5	5.9	89.7	7.4	9.44	605.6 2
Park et al.	9.5	5.9	90	7.62	9.47	613.3 4
Fafitis & Shah	9	5.9	85.7	6.5	9.52	529.6 1
Yong et al.	9.5	5.3	90.4	7	9.51	567.0 1
Mander et al.	9.6	5.75	89.5	7.9	9.32	616.7 6
Fuji et al.	10	5.7	93.4	7.75	9.34	630.9 9
Saatcioglu & Razavi	8.5	6.2	89.9	7.6	10.5	627.6
Cusson & Paoltre	14	4.54	89.96	6.43	6.42	472.9 3
Hoshikuma et al.	10	5.3	90.8	6.87	9.08	557.1
Binici	8	5.5	90.8	7.43	11.3	593.3 5
Boufia et al.	10	5.4	91.6	7.35	9.16	587.9 1
Khaje Samani & Attard	9.5	5.4	87.7	7.22	9.23	553.5 3

As it shown, ductility ratio ($\mu = \frac{\Delta_u}{\Delta_y}$) of these

models is close to each other and that of experimental specimen. The maximum difference between ductility of these analytical models and experimental frame is about 15 % and belongs to Soliman & Yu model. The average difference between ductility of the analytical models and experimental frame is about 5.5% too.

4. Discussion

3.1. Yielding Displacement

The minimum difference between yielding displacement (Δ_y) of experimental specimen and analytical models is about 1%. Yielding displacement of some models including Fafitis et al., Scout et al., Mugurama et al. and Blume et al. are very close to each other and that of experimental frame. The maximum difference is about 57% and occurs when Cusson and Paoltre model is used in analytical investigations. The average difference between yielding lateral displacement of the experimental specimen and analytical models is about 8%.

4.2. Ultimate Displacement

The maximum difference between ultimate displacement (Δ_u) of experimental specimen and analytical models is about 5% and belongs to the frame which was modeled by Fafitis et al equation. Ultimate displacements of these models are very close to each other and the average difference between the results of analytical models and that of experimental specimen is about 1%.

4.3. Yielding Load

Yielding load (P_y) of the analytical frame that was modeled by Muguruma et al.

equations is the same with experimental result. Moreover, the minimum difference between yielding load of experimental specimen and analytical models is about 2%. Yielding load of some models including Soliman et al., Sheikh & Uzumeri, Park et al., and Fafitis et al. are very close to each other and that of experimental frame. The maximum difference is about 30% and occurs when Kent & Park model is used in analytical investigations. The average difference between yielding load of the experimental specimen and analytical models is about 8%.

4.4. Ultimate Load

Ultimate load (P_u) of the analytical frame that was modeled by stress-strain equation which was developed by Fafitis et al. is very close to the experimental result and the difference is about 2%. The maximum difference is about 19% and occurs when model of Mander et al. is used in analytical investigations. The average difference between ultimate load of experimental specimen and analytical models is about 8%.

4.5. Energy Absorption

The area under the hysteresis curves of structures defined as energy absorption. But the area under the envelope curves of the structures can be used as an estimation of this parameter too. Therefore an estimation of the energy absorption of the experimental specimen and analytical models (E) are calculated and presented in Table 1. As it shown, energy absorption of the reinforced concrete frame which was analyzed by model of Khaje Samani & Attard is very close to that of experimental data and the difference is less than 1%. The maximum difference between analytical models and experimental results is about 23% and occurs when the

model of Kent & Park is used for confined concrete.

Area under the envelope curves of the analytical frames which were modeled by equations of Fuji et al., Muguruma et al. and Saatcioglu and Razavi are close to each other and subsequently, more than that of experimental results. In this case the maximum difference is about 14%.

Area under the envelope curve of the analytical frame which was modeled by equation of Cusson and Paoltreis close to that of model of Kent and Park and subsequently, less than that of experimental data. In this case the maximum difference is about 17.5%.

4.6. Tension damage and yielding pattern

Tension damage of the whole analytical models and experimental specimen are close to each other. The first tension damage appears on tension side of the columns and associated with cracking in beam-column connection. Tension damages increase with increasing the magnitude of applied lateral load and some new cracks are observed in other parts of the frame including beam and upper parts of the columns. Tension damage and yielding patterns of these analytical models are shown in Fig. 22 and Fig. 23.

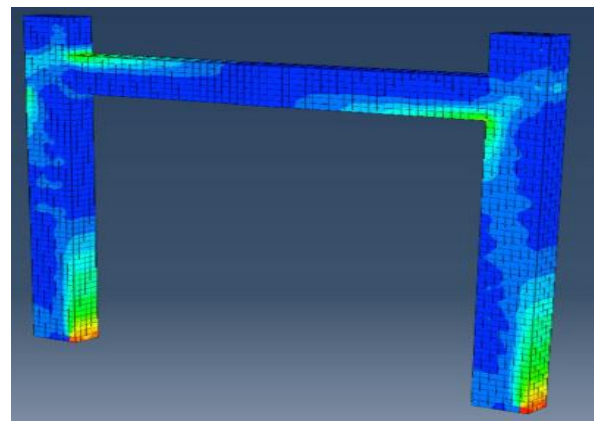


Fig. 22. Tension damage in analytical models.

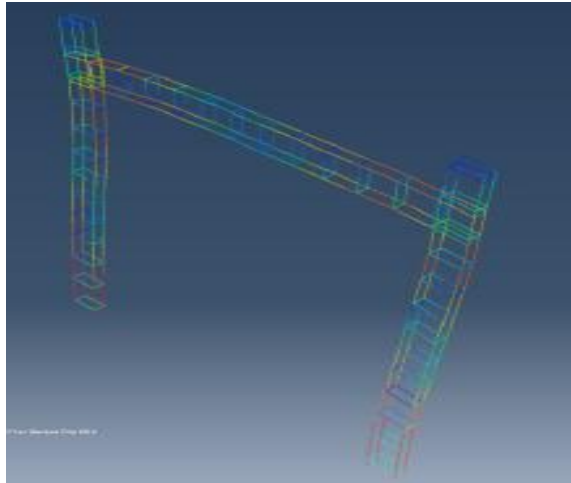


Fig. 23. Yielding pattern in analytical models.

4.6. Hysteresis Curves

Structural behavior of the analytical frame that was modeled by equation of Fafitis and Shah is very close to that of experimental data. Therefore, hysteresis curve of this model is shown in Fig.24 and compared with experimental result. As it shown, there is a good compatibility between these two curves. Envelope curves of these two models are presented in Fig.25 too.

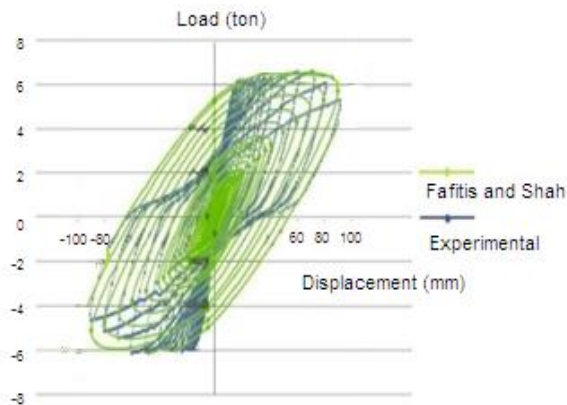


Fig. 24. Hysteresis curves of the selected analytical model and experimental results.

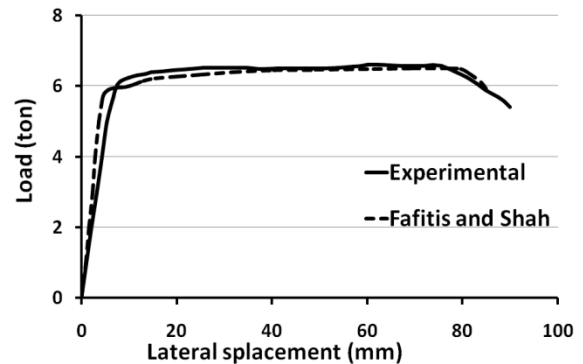


Fig. 25. Envelope curves of the selected analytical model and experimental results.

As it shown, the initial stiffness of the analytical model is more than that of experimental specimen. Yielding and ultimate displacement, yielding and ultimate load and energy absorption of these two models are very close to each other and the difference is less than 5%. It seems that, the equations which were developed by Fafitis and Shah is suitable for modeling of the confined concrete.

5. Conclusion

Based on the analytical and experimental results, the following conclusions can be drawn:

1- Longitudinal and transverse reinforcements have a confinement effect on stress-strain curve of the concrete and were investigated by different researchers. This confined concrete has more compressive stress and ultimate strain that of unconfined concrete. But the transverse reinforcement is more effective than longitudinal reinforcement.

2- All of the envelope curves which were obtained by different models had a similar linear behavior with experimental specimen.

3- Tension damage and yielding patterns of the whole analytical frames with different analytical models are close to each other and those of the experimental frame.

4- In the case of lateral load and displacement, the analytical models which were presented by Fafitis and Shah and Muguruma et al. had more compatibility with experimental results.

5- In the case of trend of the envelope curves and energy absorption, the analytical models which were presented by Khaje Samani & Attard, Yong et al. and Valenaset al. had more compatibility with experimental results.

6- In the case of yielding displacement, the maximum difference is about 57% and occurs when Cusson and Paoltre model is used in analytical investigations. In the case of ultimate load, the maximum difference is about 19% and occurs when model of Mander et al. is used in analytical investigations. Energy absorption of the reinforced concrete frame which was analyzed by model of Khaje Samani & Attard is very close to that of experimental data and the difference is less than 1%.

7- The analytical model which was simulated by equation of Fafitis and Shah has a good compatibility with experimental results. The maximum difference between the yielding and ultimate load and displacement of this analytical model and experimental data is less than 5%.

REFERENCES

- [1] Naderpour, H., Kheyroddin A., Ghodrati Amiri, G. (2010). "Prediction of FRP-confined compressive strength of concrete using artificial neural networks." *Composite Structures*, Vol. 92, pp. 2817–2829.
- [2] Wu, Y.F., Wei, Y. (2015). "General stress-strain model for steel and FRP confined concrete." *Journal of Composite for Construction*, Vol. 19, Issue 4.
- [3] Tasnimi, A.A. (2001). "Seismic behavior and design of reinforced concrete buildings." Building and Housing Research Center, Tehran, (in persian).
- [4] Suzuki, M., Akiyama, M., Hong, K.N., Cameron, I., Wang, W.L. (2004). "Stress-strain model of high strength concrete confined by rectangular ties." 13th World Conference on Earthquake Engineering, Vancouver.
- [5] Cao, V.V., Ronagh, H.R. (2013). "A model for damage analysis of concrete." *Advances in Concrete Construction*, Vol. 1, Issue 2, pp. 187-200.
- [6] Sadeghi, K. (2014). "Analytical stress-strain model and damage index for confined and unconfined concrete to simulate RC structures under seismic loading." *International Journal of Civil Engineering*, Vol. 12, Issue 3, pp. 333–343.
- [7] Naderpour, H., Kheyroddin, A., Ahmadi, M. (2014). "Compressive strength of confined concrete in CCFST columns." *Journal of Rehabilitation in Civil Engineering*, Vol. 2, Issue 1, pp. 106-113.
- [8] Campione, G., Cavaleri, L., Ferrotto, M.F., Macaluso, G., Papia, M. (2016). "Efficiency of stress-strain models of confined concrete with and without steel jacketing to reproduce experimental results." *The Open Construction and Building Technology Journal*, Vol. 10, pp. 231-248.
- [9] Larsen, N., Erduran, E., Kaynia, A.M. (2017). "Evaluation of effect of confinement on the collapse probability of reinforced concrete frames subjected to earthquakes." *Procedia Engineering*, Vol. 199, pp. 784-789.
- [10] Blume, J.A., Newmark, N.M., Corning, L.H. (1961). "Design of multistory reinforced concrete buildings for earthquake motions." *Portland Cement Association*, Chicago.

- [11] Soliman, M.T.M., Yu, C.W. (1967). "The flexural stress-strain relationship for concrete confined by rectangular transverse reinforcement." *Mag. Concrete Res.*, Vol. 19, Issue 61, pp. 223-238.
- [12] Kent, D.C., Park, R. (2016). "Flexural members with confined concrete." *J. Struct. Division*, Vol. 97, Issue 7, pp. 1969-1990.
- [13] Valenas, J., Bertero V.V., Popov, E.P. (1977). "Concrete confined by rectangular hoops and subjected to axial loads." Report No. UCB/EERC/7713, University of California.
- [14] Muguruma, H., Watanabe, S., Katsuta, S., Tanaka, S. (1980). "A stress-strain model of confined concrete." *JCA Cement and Concrete*, Tokyo, pp. 429-432.
- [15] Scott, B.D., Park, R., Priestley, M.J.N. (1982). "Stress-strain behavior of concrete confined by overlapping hoops at low and high strain rates." *ACI J.*, Vol. 79, Issue 1, pp. 13-27.
- [16] Sheikh, S.A., Uzumeri, S.M. (1982). "Analytical model for concrete confinement in tied columns." *J. Struct. Division*, Vol. 108, Issue 12, pp. 2703-2722.
- [17] Park, R., Priestley, M.J.N., Gill, W.D. (1982). "Ductility of square-confined concrete columns." *J. Struct. Division*, Vol. 108, pp. 929-950.
- [18] Fafitis, A., Shah, S.P. (1985). "Predictions of ultimate behavior of confined columns subjected to large deformations." *J. Am. Concret. Inst.*, Vol. 82, pp. 423-433.
- [19] Yong, Y.K., Nour, M.G., Nawy, E.G. (1988). "Behavior of laterally confined high-strength concrete under axial loads." *Journal of Structural Engineering*, Vol. 114, pp. 333-351.
- [20] Mander, J.B., Priestley, M.J.N., Park, R. (1988). "Theoretical stress-strain model for confined concrete." *Journal of Structural Engineering*, Vol. 114, pp. 1804-1826.
- [21] Fujii, M., Kobayashi, K., Miyagawa, T., Inoue, S., Matsumoto, T. (1988). "A study on the application of a stress-strain relation of confined concrete." *JCA Cement and Concrete*, Tokyo, pp. 311-314.
- [22] Saatcioglu, M., Razavi, S.R. (1992). "Strength and ductility of confined concrete." *Journal of the Structural Division ASCE*, Vol. 118, Issue ST6, pp. 1590-1607.
- [23] Cusson, D., Paoltre, P. (1995). "Stress-strain model for confined high-strength concrete." *Journal of Structural Engineering*, Vol. 121, pp. 468-477.
- [24] Hoshikuma, J., Kawashima, K., Nagaya, K., Taylor, A.W. (1997). "Stress-strain model for confined reinforced concrete in bridge piers." *Journal of Structural Engineering*, Vol. 123, Issue 5.
- [25] Binici, R. (2005). "An analytical model for stress-strain behavior of confined concrete." *Engineering Structures*, Vol. 27, Issue 7, pp. 1040-1051.
- [26] Bouafia, Y., Idir, A., Kachi, M.S. (2010). "Influence of the taking account of the confined concrete on the structures nonlinear calculation." *ACMA, Morocco*.
- [27] KhajeSamani, A., Attard, M.M. (2012). "A stress-strain model for uniaxial and confined concrete under compression." *J. Am. Concret. Inst.*, Vol. 41, pp. 335-349.
- [28] Tawfik, A.S., Badr, M.R., Elzanaty, A. (2013). "Behavior and ductility of high strength reinforced concrete frames." *HBRC Journal*.
- [29] Shayanfar, M.A., Kheyroddin, A., Mirza, M.S. (1997). "Element size effect in nonlinear analysis of reinforced concrete members." *Computer and Structures*, Vol. 62, Issue 2, pp. 339-352.